Numerical simulation of a Penning trap

Alessio Canclini, Filip von der Lippe
(Dated: October 23, 2022)

NB! ABSTRACT HERE

I. INTRODUCTION

The purpose of this report is to present the study of the effects of a Penning trap through numerical simulations. The Penning trap is a device used to store or "trap" charged particles using static electric and magnetic fields as shown in figure 1. These particles can then be used for a variety of experiments. Examples of this are the ALPHA, AEgIS and BASE experiments at CERN, these use Penning traps to control antimatter. The electric field is generated by two end caps (a), at the top and bottom, and a ring (b) (figure 1 only shows the ring cross-section). This electric field restricts the particles' movement in the z direction and the additional homogenous magnetic field hiders particles escaping in the xy-plane (radial direction) if it is strong enough. The magnetic field is set by a cylinder magnet (c) (figure 1 again only shows the ring cross-section).

Materials to construct a physical Penning trap are very costly, we will therefore be using a numerical approach to simulate a Penning trap. To implement such a simulation we will be working with a system of coupled non-linear differential equations. These are very difficult and often impossible to solve analytically. In addition to the material cost, the complexity of the equations therefore also motivates the use of numerical methods.

MAIN PURPOSE?

Section II will describe the mathematical and physical background as well as concrete algorithms which in this case will be implemented in C++, but can be written in any programming language.

In section III we present a selection of results form different simulations and error analysis. This will include simulations with a single particle, 2 particles and 100 random particles.

A detailed discussion of the algorithms' and results is presented in section IV, followed by a summary and potential for further experiments in section V.
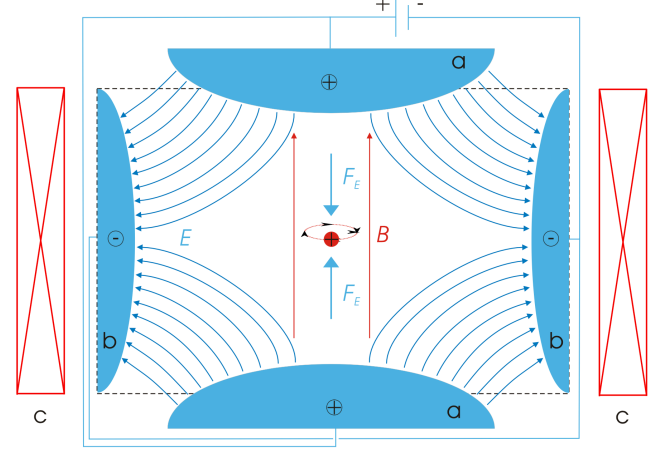

FIG. 1. This figure shows the idea of a Penning trap with a red positively charged particle in the center. Here blue lines represent the electric field generated by a quadrupole consisting of end caps (a) and a ring electrode (b). The red lines represent the magnetic field created by a surrounding cylinder magnet (c). Illustration by Arian Kriesch taken from Wikimedia Commons.

II. METHODS

The physical laws used to implement the Penning trap simulation will be from electrodynamics and classical mechanics, we will not take quantum aspects into account. The following equations will be used:

$$\mathbf{E} = -\nabla V \tag{1}$$

$\mathbf{E}$ is the electric field and V the electric potential.

$$\mathbf{E}(\mathbf{r}) = k_e \sum_{j=1}^{n} q_j \frac{\mathbf{r} - \mathbf{r}_j}{|\mathbf{r} - \mathbf{r}_j|^3} \tag{2}$$

$\mathbf{E}(\mathbf{r})$ is the electric field at a point $\mathbf{r}$. This is set up by point charges $q_1, ..., q_n$ at points $\mathbf{r}_1, ..., \mathbf{r}_n$. This comes from **Coulomb's law**, stating the magnitude of force between to point charges. $k_e \approx 8.988 \cdot 10^9 Nm^2C^{-2}$ is the Coulomb constant.

$$\mathbf{F} = q\mathbf{E} + q\mathbf{v} \times \mathbf{B} \tag{3}$$

This is the **Lonretz force**, the force $\mathbf{F}$ on a particle with charge q, an electric field $\mathbf{E}$, magnetic field $\mathbf{B}$ and velocity of the particle $\mathbf{v}$.

$$m\ddot{\mathbf{r}} = \sum_i \mathbf{F}_i \tag{4}$$

Eq. 4 is Newton's second law. Here m is the mass of the particle and $\ddot{\mathbf{r}} \equiv \frac{d^2\mathbf{r}}{dt^2}$ (the acceleration). Famously expressing that the sum of forces equals mass times acceleration.

$$V(x,y,z) = \frac{V_0}{2d^2}(2z^2 - x^2 - y^2) \tag{5}$$

For this experiment we will be considering an ideal Penning trap for which the electric field $\mathbf{E}$ is given by the electric potential V. Here V_0 is the potential applied to the electrodes. The trap will be approximated as a sphere where $d = \sqrt{z_0^2 + r_0^2/2}$ is the *charchteristic dimension* representing the length scale (or radius of the sphere) for the region between electrodes. Here z_0 is the distance from the center to the end caps (a) and r_0 is the distance from the center to the surrounding ring (b).

$$\mathbf{B} = B_0\hat{e}_z = (0,0,B_0) \tag{6}$$

$\mathbf{B}$ is the homogenous magnetic field and is dictated by the field strength B_0. With $B_0 > 0$.

Equations for single particle motion

Now starting from Newton's second law and using the equations above we can express the time evolution of a single particle's motion. The sum of forces will be the Lonretz force. Putting eq. 3 into eq. 4 leads to:

$$m\ddot{\mathbf{r}} = q\mathbf{E} + q\mathbf{v} \times \mathbf{B} \tag{7}$$

Here $\ddot{\mathbf{r}} = (\ddot{x}, \ddot{y}, \ddot{z})$ and $\mathbf{v} = (\dot{x}, \dot{y}, \dot{z})$. Putting eq. 5 into eq. 1 gives us:

$$\mathbf{E} = \left(x\frac{v_0}{d^2}, y\frac{v_0}{d^2}, -2z\frac{v_0}{d^2} \right) \tag{8}$$

Now looking at $q\mathbf{v} \times \mathbf{B}$ we have:

$$(q\dot{x}, q\dot{y}, q\dot{z}) \times (0,0,B_0) = (B_0 q\dot{y}, -B_0 q\dot{x}, 0) \tag{9}$$

Finally substituting for $\mathbf{E}$ and $q\mathbf{v} \times \mathbf{B}$ in eq. 7 results in:

$$m\begin{pmatrix} \ddot{x} \\ \ddot{y} \\ \ddot{z} \end{pmatrix} = \begin{pmatrix} qx\frac{v_0}{d^2} \\ qy\frac{v_0}{d^2} \\ -2qz\frac{v_0}{d^2} \end{pmatrix} + \begin{pmatrix} B_0 q\dot{y} \\ -B_0 q\dot{x} \\ 0 \end{pmatrix}$$

Rewriting this as a set of equations leaves us with:

$$\ddot{x} - w_0\dot{y} - \frac{1}{2}w_z^2 x = 0 \tag{10}$$

$$\ddot{y} + w_0\dot{x} - \frac{1}{2}w_z^2 y = 0 \tag{11}$$

$$\ddot{z} + w_z^2 z = 0 \tag{12}$$

Where $w_0 = \frac{qB_0}{m}$ and $w_z^2 = \frac{2qV_0}{md^2}$. Taking a closer look at eq. 12 we see that the general solution is:

$$z = A\cos(w_z^2 t) + B\sin(w_z^2 t) \tag{13}$$

eq. 10 and 11 are coupled, thus introducing a challenge. This can be resolved by introducing a complex function $f(t) = x(t) + iy(t)$ and rewriting them as a single differential equation. By introducing the complex function we have:

$$f(t) = x(t) + iy(t) \tag{14}$$

$$\dot{f}(t) = \dot{x}(t) + i\dot{y}(t) \tag{15}$$

$$\ddot{f}(t) = \ddot{x}(t) + i\ddot{y}(t) \tag{16}$$

Now multiplying eq. 11 by i gives:

$$i\ddot{y} + iw_0\dot{x} - i\frac{1}{2}w_z^2 y = 0 \tag{17}$$

eq. 10 and 17 can then be summed:

$$\ddot{x} + i\ddot{y} - w_0\dot{y} + iw_0\dot{x} - \frac{1}{2}w_z^2 x - i\frac{1}{2}w_z^2 y = 0 \tag{18}$$

Finally, substituting for $f(t)$, $\dot{f}(t)$ and $\ddot{f}(t)$ shows that eq. 10 and 11 can be rewritten as a single differential equation for f:

$$\ddot{f} + iw_0\dot{f} - \frac{1}{2}w_z^2 f = 0 \tag{19}$$

The general solution to eq. 19 is:

$$f(t) = A_+ e^{-i(w_+ t + \phi_+)} + A_- e^{-i(w_- t + \phi_-)} \tag{20}$$

where the amplitudes A_+ and A_- are positive, ϕ_+ and ϕ_- are constant phases, and

$$w_\pm = \frac{w_0 \pm \sqrt{w_0^2 - 2w_z^2}}{2} \tag{21}$$

To obtain a bounded solution for the radial movement (xy-plane) of the particle we need to introduce some constraints on w_0 and w_z. In other words we will introduce some constraints that will ensure that $|f(t)| < \infty$ as $t \to \infty$.

Studying eq. 20 one notices that $|f(t)| \to \infty$ only if $w_\pm$ is complex. To avoid this, we introduce the limitation $w_0^2 - 2w_z^2 \geq 0$, avoiding any negative values inside the square root and consequently limiting the result to real numbers. Rearranging this and remembering that $w_0 = \frac{qB_0}{m}$ and $w_z^2 = \frac{2qV_0}{md^2}$ leaves us with:

$$\frac{q}{m} \geq \frac{4V_0}{B_0^2 d^2} \tag{22}$$

A constraint, that if satisfied, keeps the particle within the Penning trap.

Now to express the upper and lower bounds of the particles' distance from the origin in the xy-plane we start

with eq. 20. Through Taylor expansion of e^{ix} we arrive at Euler's formula:

$$e^{ix} = \cos(x) + i\sin(x)$$

Introducing $u = w_+t + \phi_+$ and $v = w_-t + \phi_-$, and using Euler's formula, eq. 20 can be rewritten as:

$$f(t) = A_+\left(\cos(u) - i\sin(u)\right) + A_-\left(\cos(v) - i\sin(v)\right)$$

The physical coordinates can then be found as $x(t) = \operatorname{Re} f(t)$ and $y(t) = \operatorname{Im} f(t)$. Giving us:

$$x(t) = A_+\cos(u) + A_-\cos(v)$$
$$y(t) = -A_+\sin(u) - A_-\sin(v)$$

Since our xy-plane is a circle, the particle's distance from the origin can be expressed as the radius $R = \sqrt{x^2 + y^2}$. Substituting for x and y we have:

$$R = [(A_+\cos(u) + A_-\cos(v))^2 + (-A_+\sin(u) - A_-\sin(v))^2]^{1/2}$$

After expanding and rearranging we have:

$$R = [A_+^2(\cos^2(u) + \sin^2(u)) + A_-^2(\cos^2(v) + \sin^2(v)) + 2A_+A_-(cos(u)\cos(v) + \sin(u)\sin(v))]^{1/2}$$

Recognizing that $cos^2(u) + \sin^2(u) = 1$ and $cos(u)\cos(v) + \sin(u)\sin(v) = \cos(u-v)$ this can be simplified to:

$$R = \sqrt{A_+^2 + A_-^2 + 2A_+A_-\cos(u-v)}$$

We know that cos is a function with an upper bound of 1 and lower bound of -1. The possible bounds for R are consequently:

$$R_+ = \sqrt{A_+^2 + 2A_+A_- + A_-^2} = A_+ + A_-$$
$$R_- = \sqrt{A_+^2 - 2A_+A_- + A_-^2} = |A_+ - A_-|$$

Equations for multiple particle motion

For all simulations with more than one particle (when particle interaction is taken into account) the equations of motion will be coupled because of the Coulomb force between two point charges. Our numerical algorithms will therefore be solving the following equations:

$$\ddot{x}_i - w_{0,i}\dot{y}_i - \frac{1}{2}w_{z,i}^2 x_i - k_e\frac{q_i}{m_i}\sum_{j\neq i}^{n} q_j\frac{x_i - x_j}{|\mathbf{r}_i - \mathbf{r}_j|^3} = 0 \quad (23)$$

$$\ddot{y}_i + w_{0,i}\dot{x}_i - \frac{1}{2}w_{z,i}^2 y_i - k_e\frac{q_i}{m_i}\sum_{j\neq i}^{n} q_j\frac{y_i - y_j}{|\mathbf{r}_i - \mathbf{r}_j|^3} = 0 \quad (24)$$

$$\ddot{z}_i + w_{z,i}^2 z_i - k_e\frac{q_i}{m_i}\sum_{j\neq i}^{n} q_j\frac{z_i - z_j}{|\mathbf{r}_i - \mathbf{r}_j|^3} = 0 \quad (25)$$

Here the summation term is the Coulomb force and i and j are particle indices for n particles with charges $\{q_1, ..., q_n\}$ and masses $\{m_1, .., m_n\}$.

The algorithms

To evolve our Penning trap system in time the following algorithms will be implemented to solve our particles' equations of motion. Consider the forward difference approximation for the first derivative based on Taylor expansion

$$y_n' = \frac{y_{n+1} - y_n}{h}, \quad h = t_{t-1} - t_n \quad (26)$$

Rearranging this results in the forward Euler method which has a Global error of $\mathcal{O}(h)$, making it only first order accurate. The method is easy to implement and will be used for comparisons and checking of the main algorithm.

Algorithm 1 Forward Euler method

procedure FORWARD EULER(y_0, h)
  $y' = f(t_i, y_i)$ ▷ Single fist-order diff. eq.
  $n = 1/h$ ▷ Compute number of steps

  for $i = 0, 1, 2, \ldots, n$ **do**
    $y_{i+1} = y_i + hf(t_i, y_i)$ ▷ Value at next time step

Similarly to the forward Euler, Runge-Kutta fourth order (RK4) is based on Taylor expansion, but by adding several intermediate steps to the computation of y_{i+1} it generally yields better solutions for ODEs. RK4 has a global error of $\mathcal{O}(h^4)$.

Algorithm 2 Runge-Kutta fourth order method

procedure RUNGE-KUTTA FOURTH ORDER(y_0, h)
  $y' = f(t_i, y_i)$ ▷ Single fist-order diff. eq.
  $n = 1/h$ ▷ Compute number of steps

  for $i = 0, 1, 2, \ldots, n$ **do**
    $k_1 = hf(t_i, y_i)$ ▷ Intermediate step 1
    $k_2 = hf(t_i + h/2, y_i + k_1/2)$ ▷ Intermediate step 2
    $k_3 = hf(t_i + h/2, y_i + k_2/2)$ ▷ Intermediate step 3
    $k_4 = hf(t_i + h, y_i + k_3)$ ▷ Intermediate step 4
    $y_{i+1} = y_i + \frac{1}{6}(k_1 + 2k_2 + 2k_3 + k_4)$ ▷ Final algorithm

---

The RK4 scheme will be our main method as this is a "gold standard" in numerical analysis. Early tests with one single particle will be confirmed by an analytical solution, but for comparison of more complex scenarios the simple forward Euler scheme will also be implemented.

The Penning trap with time evolving algorithms will be implemented in an object-oriented C++ code, the plots are generated using Python.

Particles

Our charged particles will be singly-charged Calcium ions (Ca^+) with a mass of $40.077u$.

- Particle 1:
$$(x_0, y_0, z_0) = (20, 0, 20)\mu m$$
$$(v_{x,0}, v_{y,0}, v_{z,0}) = (0, 25, 0)\mu m/\mu s$$

- Particle 2:
$$(x_0, y_0, z_0) = (25, 25, 0)\mu m$$
$$(v_{x,0}, v_{y,0}, v_{z,0}) = (0, 40, 5)\mu m/\mu s$$

Simulations with one particle will use Particle 1 whilst simulations with two particles will use both Particle 1 and Particle 2. For further simulations with 100 particles, Armadillo's `vec::randu()` function will be used to generate random initial positions and velocities for each particle.

Numbers and units

III.   RESULTS

First we test our Penning trap's behavior for a single particle to see if it produces the expected motion in this simple case. All three solutions have been plotted in figure 2 to examine weather the numerical and analytic results agree.
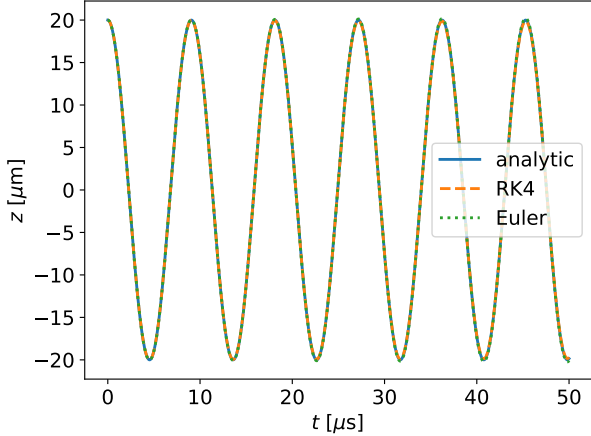
FIG. 2. Here we see the vertical path of a single particle over 50 μs. The analytic, Euler and RK4 solutions are shown.

Figure 2 shows that both the forward Euler and RK4 method show the same z motion as the analytic solution for a single particle. The particle oscillates vertically.
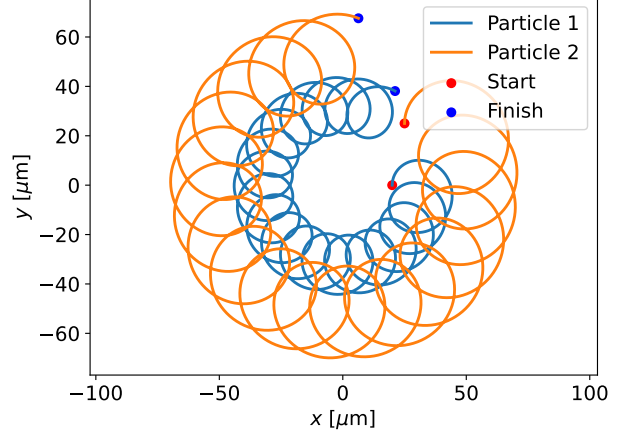

FIG. 3. The horizontal (xy-plane) path of two particles without interaction.

In figure 3 we see the motion of Particle 1 and Particle 2 in the xy-plane when they do not interact. That is, disregarding the Coulomb force. The paths have a very similar spiraling shape both resulting circular patterns around the origin.
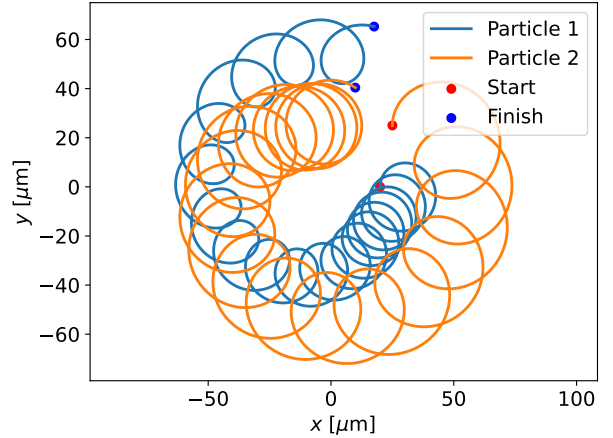

FIG. 4. The horizontal (xy-plane) path of two particles with interaction.

Figure 4 shows the same two particles as figure 3 with the exact same initial conditions, but with interaction between particles. We notice that the paths, although still spiraling, are not as circular.
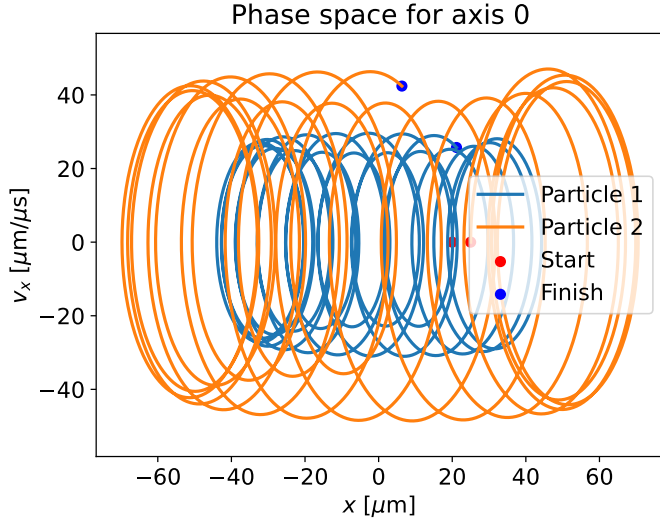
FIG. 5. The phase space (x, v_x) of two particles without interaction.
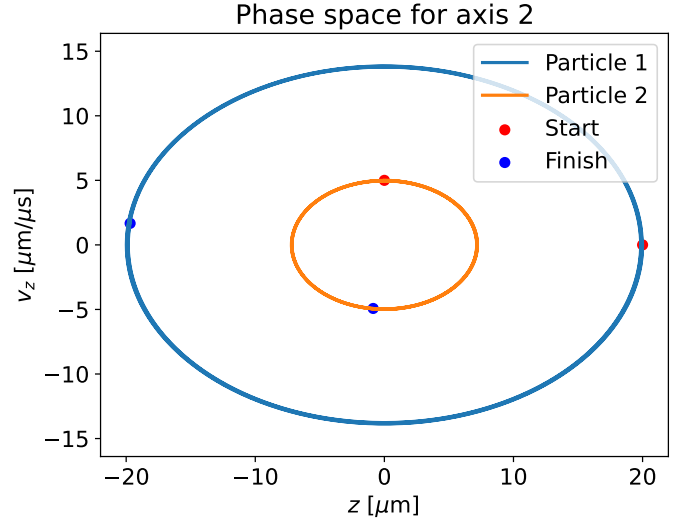

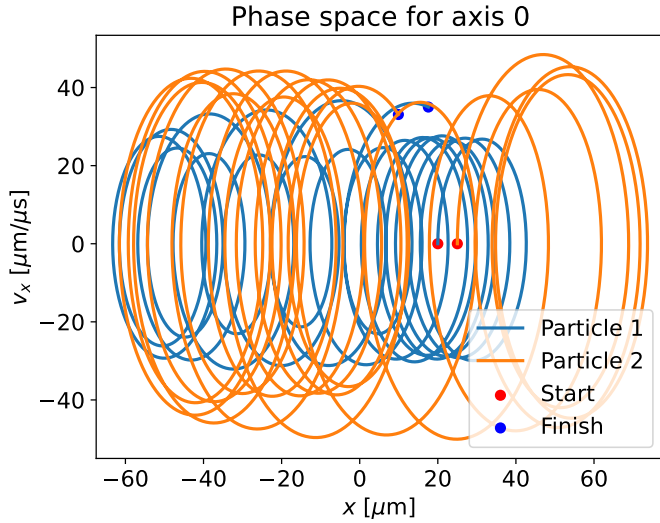FIG. 7. The phase space (z, v_z) of two particles without interaction.

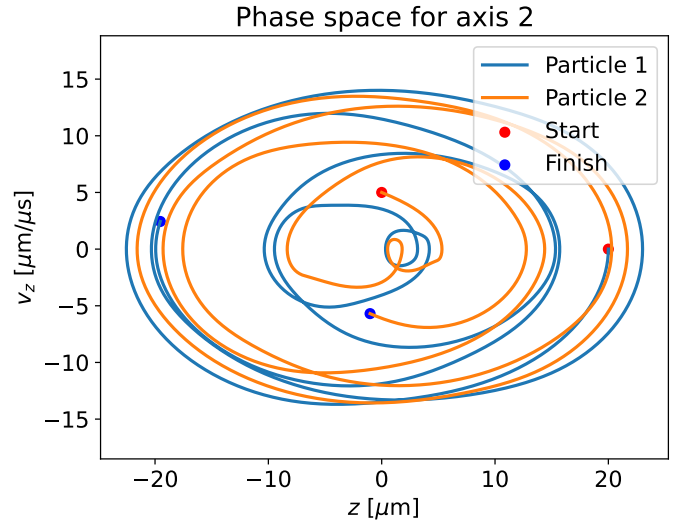FIG. 6. The phase space (x, v_x) of two particles with interaction.

FIG. 8. The phase space (z, v_z) of two particles with interaction.

The two figures above show the trajectories of Particle 1 and Particle 2 in the (x, v_x) plane. Figure 5 is a simulation disregarding particle interaction whilst figure 6 shows the trajectories with particle interaction. We notice that the trajectories in figure 5 are fairly repetitive whilst figure 6 shows more variations and different final points to figure 5.

Figures 7 and 8 show the trajectories of Particle 1 and Particle 2 in the (z, v_z) plane. In figure 7, without particle interactions, we notice what seems to be repetitive trajectories similarly to figure 5. Figure 8 which includes particle interactions on the other hand displays more irregular trajectories similarly to figure 6.
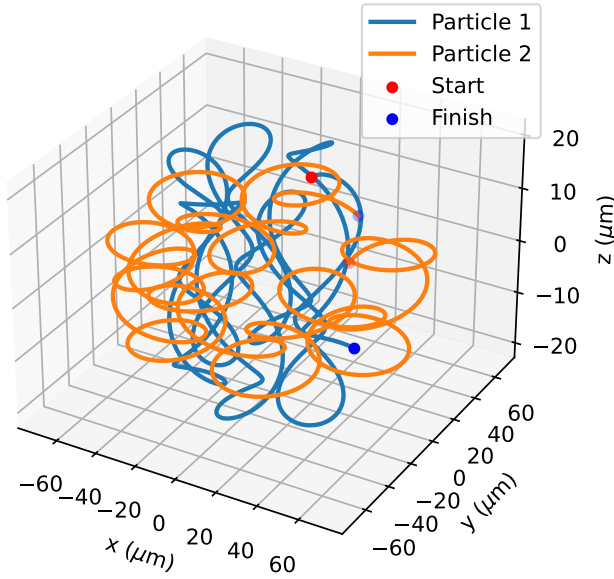
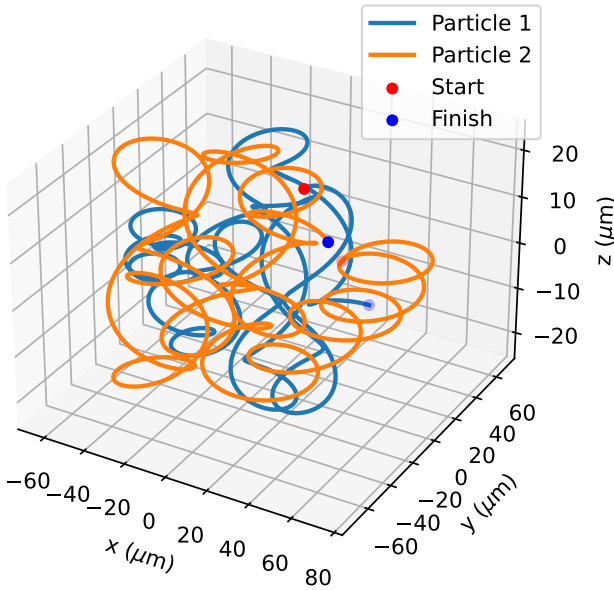FIG. 9. Shows a 3D representation of two particle paths without interaction.

FIG. 11. The plot shows the relative error for a single particle's motion over 50 μs using the forward Euler approximation. The four different lines show results for different step sizes $h = 50/N\mu s$

FIG. 10. Shows a 3D representation of two particle paths with interaction.

FIG. 12. The plot shows the relative error for a single particle's motion over 50 μs using the fourth order Runge-Kutta approximation. The four different lines show results for different step sizes $h = 50/N\mu s$

Looking at the 3D-plots in figures 9 and 10 it is difficult to follow the exact motion of the particles. Comparing figure 9, without particle interactions, to figure 10, with interactions, one notices that the start positions are identical, yet the finishing positions differ. Taking a close look it is also possible to see differences in the orange and blue lines in the two figures.
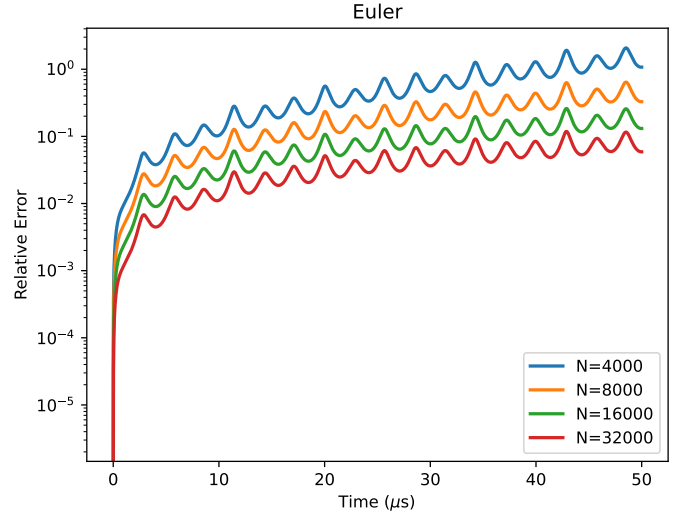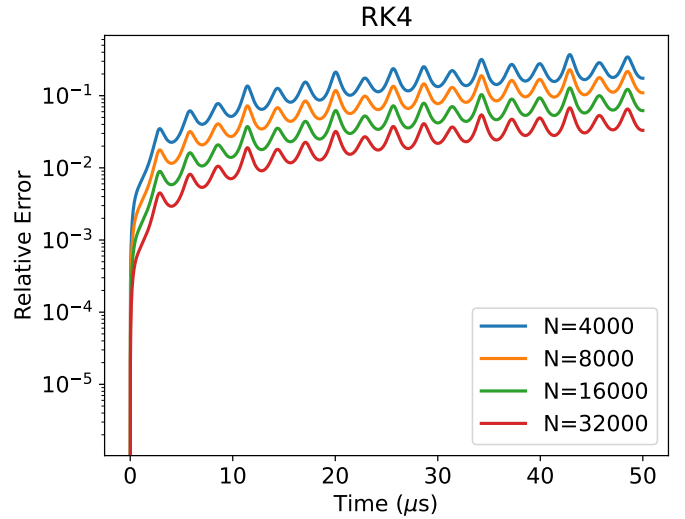
Considering the case of a single particle to allow for a comparison to the analytic solution, figures 11 and 12 display the relative error of the forward Euler method (figure 11) and the RK4 method (figure 12) for different step sizes $h = 50/N\mu s$. Noticeably for both methods, the error decreases as the step size does too (increasing the number of points N). Comparing the two, one clearly sees that the RK4 method is more precise than the forward Euler.

IV.   DISCUSSION

Note that you are free to merge the presentation and discussion of the results into a single section of your report. This can in many cases lead to a more fluid presentation. If you do this, we recommend you use "Results and discussion" or similar for the section title.

From table **??**, we note that our implementation reproduces the analytical results to four digits precision when the integration range is divided into $n = 10^4$ subintervals. This indicates that that our implementation of the algorithm is correct.

From figure **??**, we see that $\log_{10}(\epsilon)$ decreases linearly with $\log_2(n)$. From this, it should be possible to extract the convergence rate of our implementation of the midpoint rule. From a theoretical point of view we know that the midpoint rule should have a convergence rate of $\mathcal{O}(h^2)$. To properly verify our implementation, we should have estimated the convergence rate from our results and compared it to this theoretical rate. Without doing so, we cannot know that the our implementation of the algorithm is correct, even though we have seen that the numerical approximation converges to the correct answer in **??**.

Although this is a somewhat silly example, please note the following: We are to-the-point in our discussion of the results, and we only make strong claims about what we are actually certain about. In the discussion it is important to try to be as concise as possible — long paragraphs that only make very general points are typically of limited interest. Note that we also highlight aspects of our analysis that could have been improved and that might form a topic for future work.

V.   CONCLUSION

In this section we state three things in a concise manner: what we have done, what we have found, and what should or could be done in the future.

We have investigated an implementation of the midpoint rule for numerical integration. As a first validation test we have checked that our implementation of the method reproduces the analytical result for the definite integral of $f(x) = x^3$ on $x \in [0, 1]$, achieving a four-digit precision when the integration range is divided into $n = 10^4$ subintervals. Furthermore, we have presented results for how the relative error of the method varies with the number of subintervals. To use these results to extract a precise estimate for the convergence rate of the method remains a topic for future work. As such, while our implementation of the midpoint rule has passed the initial validation tests, more work is needed to fully assess the validity of the implementation.